JOTCS A
Journal of the Turkish Chemical Society
Section: A
Chemistry

TURKISH CHEMICAL SOCIETY

Lannea microcarpa Leaves Extract as Corrosion Inhibitor for Al Metal in HCl Acid Medium

Umaru Umar[1], Abdullahi Muhammad Ayuba[1]*

[1]Bayero University, Faculty of Physical Sciences, Department of Pure and Industrial Chemistry, Kano, 700241, Nigeria.

Abstract: Techniques for weight loss, electrochemistry, scanning electron microscopy (SEM), and Fourier transform infrared spectroscopy (FTIR) were used to investigate the inhibitory impact of *Lannea microcarpa* leaves extract. The weight loss data showed that the plant extract's ability to suppress corrosion increased with higher concentrations and decreased with higher temperatures and HCl acid concentrations. According to the electrochemical data, the plant extract uses a mixed type mechanism to limit both cathodic and anodic reaction rates. Calculated activation energies were found to be higher in inhibited systems than in uninhibited systems, indicating physisorption, while negative values of ΔG point to a process that is both possible and spontaneous. The inhibitory mechanism was demonstrated by FTIR spectra to be an adsorption process through the functional groups present in the phytochemicals of the plant extract onto the surface of Al metal. SEM surface morphology study demonstrated the protection that the extract provided on the metal surface. Compared to other isotherm models that were examined, the adsorption data were found to be more reliable and suited the Langmuir isotherm well.

Keywords: Aluminium, *Lannea microcarpa*, Weight loss, Inhibition efficiency.

Submitted: October 20, 2022. **Accepted:** September 26, 2024.

Cite this: Umar U, Ayuba AM. *Lannea microcarpa* Leaves Extract as Corrosion Inhibitor for Al Metal in HCl Acid Medium. JOTCSA. 2024;11(4): 1553-64.

DOI: https://doi.org/10.18596/jotcsa.1192167

***Corresponding author's E-mail:** ayubaabdullahi@buk.edu.ng

1. INTRODUCTION

Due to their low cost, high strength, ductility, formability, durability, and conductivity, aluminium and its alloys are employed in a variety of industries and in a variety of capacities (1). Despite the fact that aluminium promotes the formation of a compact, adherent passive oxide film to protect it from corrosion in a variety of environments, this film's surface is amphoteric and dissolves significantly when the metal is exposed to strong acid or base solutions, making it susceptible to corrosion (2). Metal corrosion management can be achieved using a variety of approaches, but using inhibitors is the most efficient, secure, and cost-efficient approach (3). Due to the hazardous effects of synthetic chemicals on human and animal life during their manufacturing and usage, synthetic inhibitors are increasingly causing greater environmental problems (4). For their eco-friendliness, accessibility, cost, and effectiveness, phyto-inhibitors are now receiving more attention in the research community than their synthetic equivalents (5).

Lannea microcarpa, an African grape that is dioecious and a member of the Anacardiaceae family, is found in the Sudanian zone (6). It has a 70cm diameter and a maximum height of 15 meters. It has a spherical parasol-like top with a few branches that fall and have dense foliage (7). The species can be found over much of Nigeria and the western Sahel (typically in rocky regions with pockets of sand) (8). We have found that there is a dearth of literature on the use of *Lannea microcarpa* as a corrosion inhibitor for Al metal. This paper focuses on the application of weight loss, electrochemical, FITR and SEM techniques in using *Lannea microcarpa* leaf extract as a corrosion inhibitor for Al metal in acid solution.

2. EXPERIMENTAL SECTION

2.1. Plant Sample Collection

From the Bayero University Kano (Old campus), Gwale local government area, Kano state, Nigeria, fresh leaves of *Lannea microcarpa* were harvested. It was identified by a botanist from the Bayero University Kano's Department of Plant Biology and

given the herbarium registration number BUKHAN 280 for records and references. The leaves were then washed, let to air dry, powdered into a powder, and sieved to pass through a sieve with a mesh size of 250nm.

2.2. Plant Extraction

500 g of the sieved, powdered plant extract sample was soaked in 1.5 L of 95 percent ethanol for two weeks while being constantly stirred. Following that, the mixture was filtered and concentrated using rotavapor (BUCHI Labortechnik AG/9230 Flawil/Switzerland) to remove the extract from the ethanol. After one week of air drying, the concentrated extract was weighed and labelled for future use.

2.3. Aluminium Coupons Preparation

Al (99.36%), Si (0.02%), Fe (0.14%), S (0.04%), Cl (0.03%), K (0.03%), Cu (0.02%), Ti (0.01%), Ga (0.01%), and Mn (0.01%) are the components of the aluminium sheet employed in this investigation. The sheet was mechanically cut into coupons that were each 4 x 3 x 0.11 cm in size. Each voucher was cleaned with ethanol, dipped in acetone, left to dry in the open air to remove any remaining grease, and then preserved in a dessicator (9).

2.4. Preparation of Plant Extract Solutions

Weighing 0.2, 0.4, and 0.6 g of the extract, respectively, and dissolving each in 5 mL of ethanol, then transferring each into 1 litre of 0.2 M HCl separately and making up to the mark, were used to prepare 0.2, 0.4, and 0.6 gL^{-1} of the extract in 0.2 M HCl. The extract solutions (0.2, 0.4, and 0.6 gL^{-1}) in 0.4 and 0.6 M HCl were made using the same method. In order to balance the solutions, 5ml of ethanol was added to 0.2, 0.4, and 0.6 M HCl to create blank corrodent solutions.

2.5. Phytochemical Analysis of the Plant Extract

The ethanolic extract of *Lannea microcarpa* leaves underwent phytochemical analysis using the procedure described by Prishant *et al*. (10). Alkaloids, saponins, phytosterols, phenols, flavonoids, proteins, amino acids, and triterpenes are a few of the secondary metabolites that were examined.

2.6. Weight Loss Experiments

Aluminium coupons that had already been processed and weighed were immersed separately and completely in 100 mL beakers containing test solutions at various concentrations, both with and without the inhibitor. The beakers were sealed before being placed inside a thermostatic water bath that was kept at a specific temperature. For a total of 4 hours, the coupons were removed from the test solutions at 1-hour intervals, washed with distilled water and a soft brush, dried in acetone, and reweighed. The weight disparities were interpreted as weight reduction (11). The temperature (303, 313 and 323 K), corrodent concentration (0.2, 0.4 and 0.6 M HCl), and extract concentration (0.2, 0.4 and 0.6 g/L) were varied during the weight loss experiment. The inhibition effectiveness (%I) of the inhibitor, the degree of surface covering (θ), and the corrosion rate of the Al metal coupon (CR) were determined using equations 1-3, respectively, from the weight loss findings (12):

$$\%I = \left(1 - \frac{w_1}{w_2}\right) X\ 100 \quad (1)$$

$$\theta = 1 - \frac{w_1}{w_2} \quad (2)$$

$$CR(gh^{-1}cm^{-2})\frac{\Delta w}{At} \quad (3)$$

Where w_1 and w_2 represent the weight loss (g) of aluminium in the presence and absence of an inhibitor, respectively, in HCl solutions, θ denotes the degree of surface coverage, CR denotes the rate of corrosion, Δw denotes the weight loss (g), A denotes the area of the specimen (cm^2), and t denotes the time spent submerged (h).

2.7. Electrochemical Measurements

The electrochemical tests used Al metal samples that were 1 cm x 1 cm in size. Then, these were covered with epoxy resin, leaving only one square surface measuring 1.0 cm^2 exposed. The exposed surface underwent acetone degreasing, distilled water rinsing, and warm air drying. At a scan rate of 0.333mV per second and a temperature of 298K, linear polarization studies on uninhibited and inhibited (0.2, 0.4, and 0.6 g/L) samples in 0.2 M HCl were performed on potential ranges of -1000 to -2000 mV (13).

2.8. Fourier Transform Infrared Spectrophotometry (FT-IR) Analysis

The main functional groups in the leaves extract of *Lannea microcarpa* and the corrosion by product of inhibited Al metal in HCl solution were identified using an FT-IR instrument type Cary 630 FTIR Spetrophotometer (Agilent Technologies). The material was scanned 32 times at a resolution of 8 cm^{-1} throughout a wave number range of 650 to 4000 cm^{-1} for the analysis (14).

2.9. Scanning Electron Microscopy (SEM) Analysis

Using a scanning electron microscope, morphological analyses of the aluminium coupon surfaces exposed to uninhibited and inhibited corrosion systems (0.6 M HCl) for 4 hours at 323 K were taken (Phenom World Eindhoven). A very little amount of the materials to be examined were distributed on the stub during the sample preparation process for SEM analysis, and the stub was then viewed in the instrument to obtain micrographs at an accelerating voltage of 15.00 kV and x500 magnification (13).

3. RESULTS AND DISCUSSION

3.1. Phytochemical Screening

According to the phytochemical analysis of an ethanolic extract of *Lannea microcarpa* leaves, flavonoids, tannins, phenols, proteins, sterols, and saponins were present (Table1). The corrosion

prevention properties of plant extracts on metal surfaces have been attributed to the presence of secondary metabolites (4). The phytoconstituents in the ethanolic extract of *Lannea microcarpa* leaves are thought to have prevented aluminium from corroding because the chemical structures of the majority of these phytoconstituents contained electron-rich bonds or heteroatoms, which facilitate their ability to donate electrons. Researchers have obtained similar conclusions on the inhibition of metal corrosion by plant extracts (15–16). Additionally, Obi-Egbedi and Obot (17) reported that the presence of π-electrons or appropriate functional groups may facilitate the transfer of charge from the inhibitor's molecule to the charged metal surface (physical adsorption) or the transfer of electrons from the inhibitor's molecule to the vacant orbitals of the metal (chemical adsorption).

Table 1: Phytochemical Screening of the Leaves Extract of *Lannea macrocarpa*.

Bioactive agent	Qualitative analysis
Flavonoids	+
Phenols	+
Proteins/amino acids	+
Alkaloids	-
Saponins	+
Triterpenes	-
Phytosterols	+
Tannins	+

key: + indicates the presence of phytochemical, - indicates the absence of phytochemical.

3.2. Weight Loss Experiment Results

3.2.1. Effect of corrodent concentration

Studying the weight loss of aluminium in 0.2, 0.4, and 0.6 M HCl solutions for 4 hours at 303, 313 and 323 K examined the effect of corrodent concentration. The findings demonstrated that weight loss and the rate of corrosion in unhindered aluminium are both accelerated by an increase in acid concentration (Figure 1). The corrosion rate of aluminium in blanked 0.2 M HCl at 303 K is 0.0875 $mgh^{-1}cm^{-2}$, while that in blanked 0.6 M HCl at the same temperature is 1.8229 $mgh^{-1}cm^{-2}$, as shown in Table 2. The aforementioned finding might be explained by the fact that chemical reaction rates rise as active species concentrations do (18). In general, the presence of water, air, and H^+ is thought to speed up the corrosion process. As a result, as the acid concentration rises, the active species, H^+, rises as well, increasing the corrosion rate. The observation might possibly be the result of an increase in the rate of active species' diffusion and ionization during corrosion reactions (19).

Additionally, the increase in weight loss brought on by an increase in acid concentration on aluminium that has been inhibited may be explained by the fact that acid molecules at higher concentrations can break the bond between extract compounds and aluminium surface to form a hydrogen-aluminium bond (20), which leads to a higher accumulation of the active sites by acid molecules and prevents the penetration of extract molecules to the surface of the aluminium.

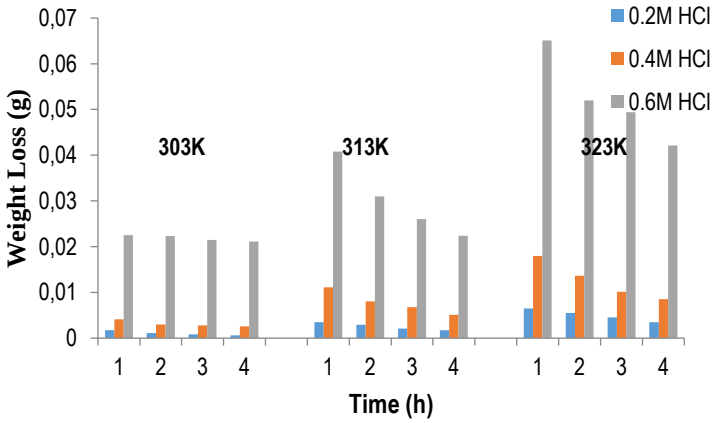

Figure 1: Variation of Weight Loss with Time for the Corrosion of Aluminium in Blank HCl at Varying Temperatures.

3.2.2. Effect of inhibitor on the corrosion process

At 303, 313 and 323 K, the influence of the inhibitor *Lannea microcarpa* at varied concentrations (0.2, 0.4 and 0.6 g/L) on the corrosion process of aluminium has been investigated. The weight loss over time of aluminium immersed in 0.2, 0.4, and 0.6 M HCl with varied extract concentrations at 303, 313 and 323 K is depicted in Figures 2a-c. The results clearly show that, in all three concentrations of HCl and at all temperatures, the weight loss of aluminium increases with increasing contact time but reduces with increasing inhibitor concentration. The findings also show that all three doses of *Lannea microcarpa* prevented aluminium corrosion in all concentrations of HCl and at all research temperatures. Table 2 showed that while surface

coverage and inhibition effectiveness increased with increasing inhibitor doses, the rate of corrosion of aluminium decreased. The inhibition efficiency rises from 57.14% to 76.19% when the inhibitor concentration is changed from 0.2 g/L to 0.6 g/L in 0.2 M HCl. This demonstrates how *Lannea microcarpa* extract can prevent aluminium from corroding in HCl solutions by acting as an inhibitor. The adsorption of extract molecules onto the Al metal, which reduces the area of contact between Al metal and corrosive media, is responsible for the decrease in weight loss and corrosion rate that is observed with increasing extract concentrations. According to Thilagavathy and Saratha (21), similar outcomes were obtained.

However, Table 2 shows that the extract's ability to prevent growth declines as temperature rises. For example, the extract's ability to inhibit growth (0.6 g/L) in 0.2 M HCl at 303 K was 76.19 %, but when the temperature was raised to 323 K under the same conditions, the effectiveness dropped to 47 % (Table 2). This shows that the physical adsorption mechanism described by Awe *et al.* (13) is consistent with the adsorption of extract of *Lannea microcarpa* on Al metal.

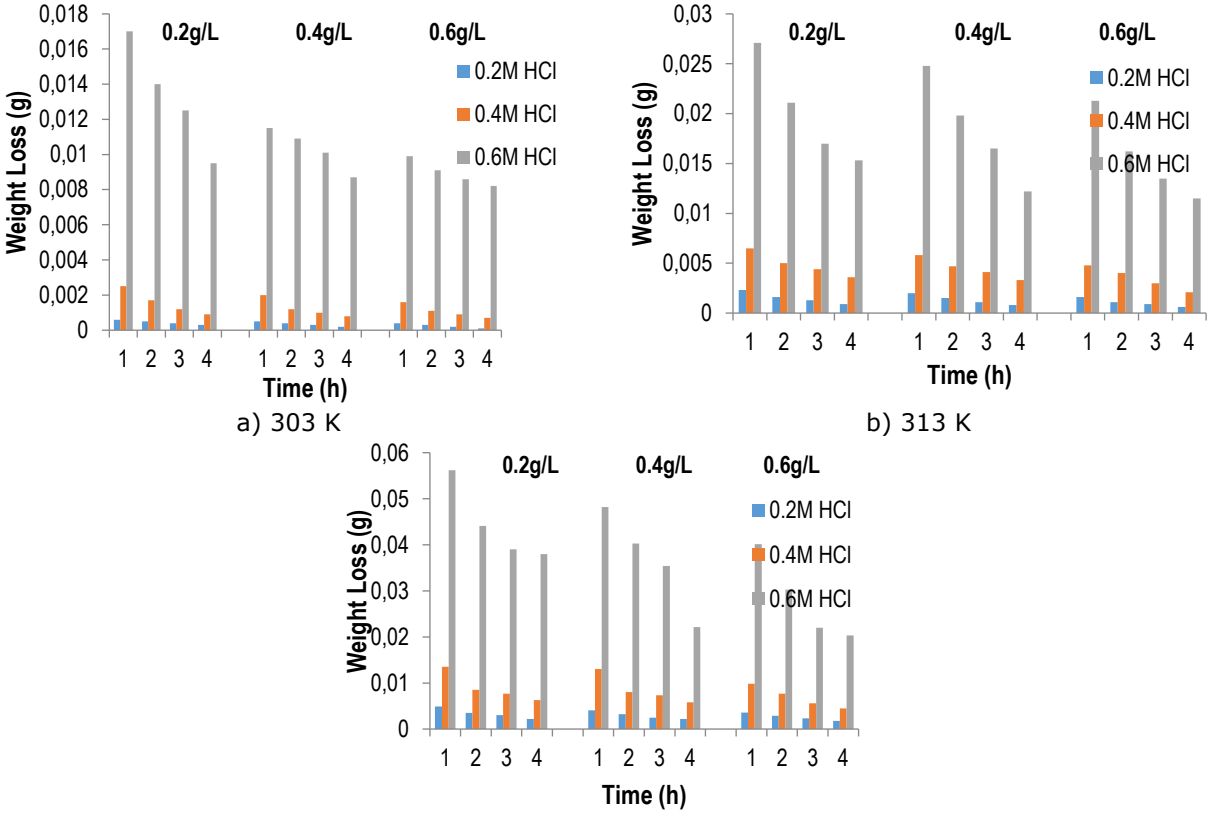

Figure 2: Variation of Weight Loss with Time of Aluminium Immersed in different Concentrations of Extract in 0.2, 0.4 and 0.6M HCl at Varying Temperatures (303, 313 and 323K).

3.2.3. Effect of temperature on the corrosion process

By adjusting the temperature (303, 313 and 323 K), it was possible to determine the impact of temperature on the weight loss and corrosion rate of Al metal immersed in 0.2, 0.4, and 0.6 M HCl for four hours. The results are shown in the Figures (3a-c). The data show that the weight loss of Al metal, both inhibited and uninhibited, increases with temperature in all three acid concentrations. Additionally, Table 2 shows that in all three acid concentrations, the corrosion rate rises with rising temperature. At 303 K, the corrosion rates of the blank and the 0.6 g/L inhibited Al metal were 0.0875 and 0.0208 mg/h.cm^2 respectively, whereas at 323 K, the rates increase to 0.4167 mg/h.cm^2 and 0.2208 mg/h.cm^2, respectively (Table 2). This observation demonstrates that a rise in temperature improves the reactivity of the corrosion medium's active ingredients. A boost in temperature typically accelerates the cathode's hydrogen evolution reaction, which raises the rate at which metals dissolve. The fact that chemical reactions intensify with rising temperature is another argument in favour of it (general rule guiding the rate of chemical reactions). Additionally, a rise in temperature boosts the kinetic energy of the molecules in the corrosion medium, allowing corrosion to more quickly overcome the energy barrier.

Table 2 also shows that inhibitory effectiveness diminishes as temperature rises. This can be ascribed to the protective coatings on the metal being more soluble, increasing the metal's sensitivity to corrosion (22). Due to the increased molecule desorption at higher temperatures, this data shows poor physical adsorption contact between the inhibitor and Al surface (23).

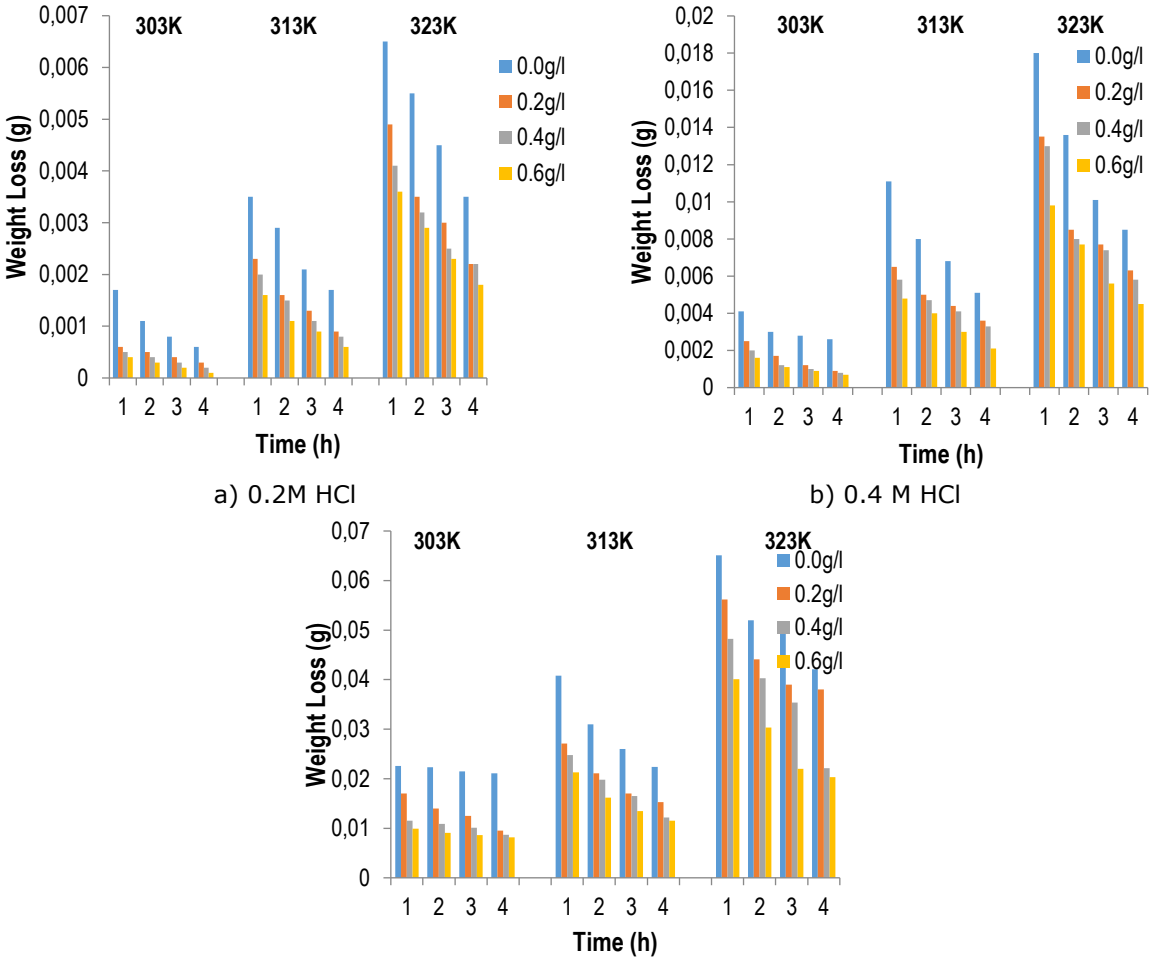

a) 0.2M HCl b) 0.4 M HCl

c) 0.6 M HCl

Figure 3: Variation of Weight Loss with Time of Aluminium Immersed in Various Concentrations of Extract at Varying HCl Concentration at 303, 313 and 323 K.

Table 2: Weight Loss Calculated Parameters of Various Concentrations of *Lannea microcarpa* Extract.

Temp. (K)	Conc. of extract (g/L)	0.2 M HCl			0.4 M HCl			0.6 M HCl		
		CR (mg/cm.h) x 10^{-2}	θ	% I (%)	CR (mg/cm.h) x 10^{-2}	θ	% I (%)	CR (mg/cm.h) x 10^{-2}	θ	% I (%)
303	0.0	8.8	-	-	26.0	-	-	182.2	-	-
	0.2	3.8	0.57	57.1	12.9	0.50	50.4	100.0	0.45	45.1
	0.4	2.9	0.67	66.7	10.6	0.59	59.2	85.8	0.53	52.9
	0.6	2.1	0.76	76.2	10.0	0.62	61.6	74.6	0.59	59.1
313	0.0	21.3	-	-	64.6	-	-	250.4	-	-
	0.2	12.7	0.40	40.2	40.6	0.37	37.1	167.7	0.33	33.0
	0.4	11.3	0.47	47.1	37.3	0.42	42.3	152.7	0.39	39.0
	0.6	8.8	0.59	58.8	28.9	0.55	55.2	130.2	0.48	48.0
323	0.0	41.7	-		104.6	-	-	434.6	-	-
	0.2	28.3	0.32	32.0	77.1	0.26	26.3	369.4	0.15	15.0
	0.4	25.0	0.40	40.0	70.8	0.32	32.3	317.1	0.27	27.0
	0.6	22.1	0.47	47.0	57.5	0.45	45.0	269.2	0.38	38.1

3.3. Polarization Measurements

Tafel's polarization curves of an aluminium electrode in 0.2 M HCl are shown in Figure 4 in both the presence and absence of various amounts of extract from *Lannea microcarpa*. The plots also show that both cathodic and anodic reactions were suppressed with the addition of various concentrations of *Lannea microcarpa*, indicating that the plant extract served as a mixed-type inhibitor, reducing the rates of both anodic dissolution and cathodic hydrogen evolution reactions. It can be seen from Figure 4 that the cathodic and anodic reactions in blank HCl follow Tafel's law.

Additionally, it can be seen from Figure 4 that the polarization plots for the inhibited electrodes don't differ significantly from those for the uninhibited electrode, indicating that the presence of *Lannea microcarpa* extract only slows down corrosion rather than changing the electrochemical reactions that

cause corrosion (24).

In Table 3, the electrochemical characteristics obtained by extrapolating Tafel lines are shown, including inhibition efficiency (IE), corrosion rate (CR), corrosion potential (E_{corr}), cathodic and anodic Tafel slopes (β_c and β_a, respectively), and corrosion current density (I_{corr}). The inhibitory efficiencies were determined using equation 4 and it was discovered that they rose as extract concentration rose (25).

$$IE(\%) = \frac{i^o_{corr} - i_{corr}}{i^o_{corr}} X\ 100 \qquad (4)$$

Where i^o_{corr} and i_{corr} are the corrosion current densities obtained from uninhibited and inhibited solutions respectively.

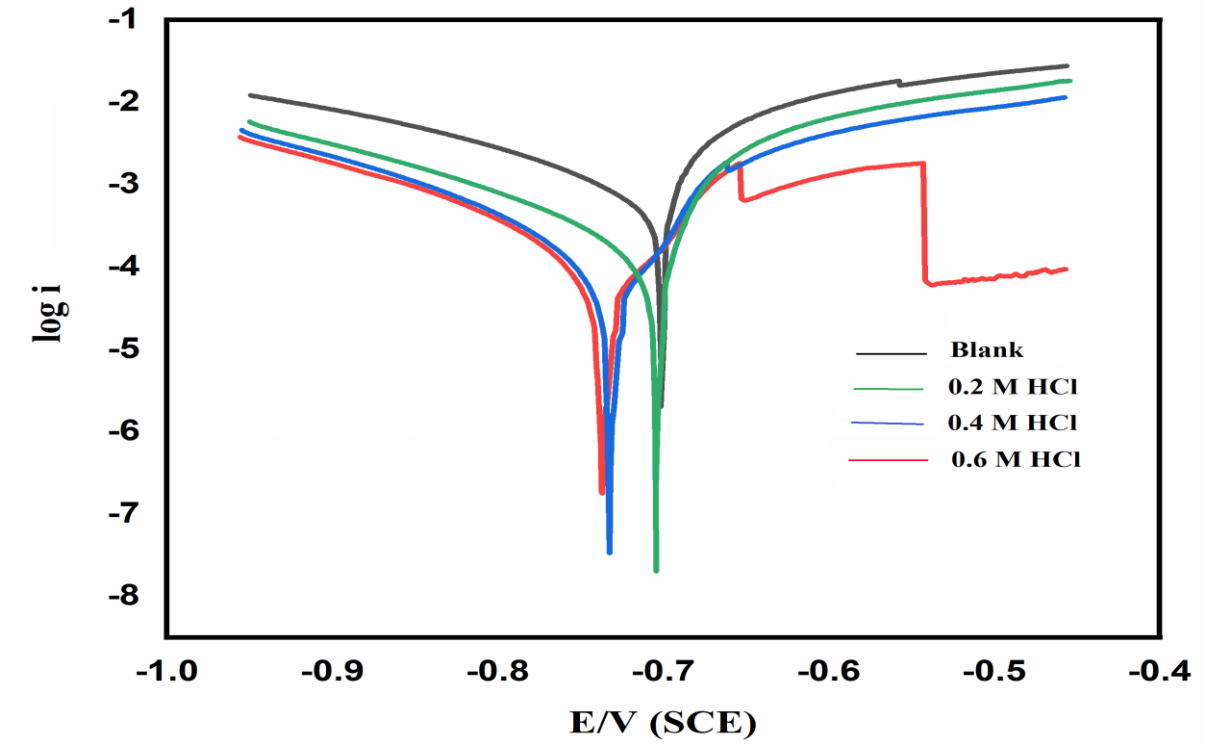

Figure 4: Overlayed Tafel Polarization Curves Recorded for Al in 0.2 M HCl Solution at Varying Concentrations of *Lannea microcarpa.*

Table 3: Electrochemical Parameters Obtained from Tafel polarization technique for Al in 0.2 M HCl Solution at Varying Concentrations of Extract at 25 °C

Extract concentration (gL^{-1})	i_{corr} (μAcm^{-2})	E_{corr} (mV)	β_a (mV dec^{-1})	β_c (mV dec^{-1})	% I (%)
0.0	-389.197	-701.151	29.996	102.27	-
0.2	-37.571	-737.556	56.091	50.156	90.35
0.4	-28.892	-730.858	37.206	53.955	92.58
0.6	-22.704	-703.843	14.729	36.837	94.17

3.4. Fourier Transform Infrared (FT-IR) Spectroscopic Results

In the images, the IR spectra of a corrosion product with an inhibitor and a powdered extract of *Lannea microcarpa* leaves are displayed (Figures 5 a-b). The C-N stretch at 1100 cm^{-1} shifts to 1112 cm^{-1}, the C-O stretch at 1153 cm^{-1} shifts to 1156 cm^{-1}, the N-O stretch at 1316 cm^{-1} changes to 1343 cm^{-1}, the C-C stretch in the ring at 1447 cm^{-1} drops down to 1410 cm^{-1}, and the N-H bend shifts from 1607 cm^{-1} to 1547 cm^{-1}, according to a comparison of the spectrum of extract and corrosion product with inhibitor. The change in frequency suggests that the metal and plant extract are interacting (26).

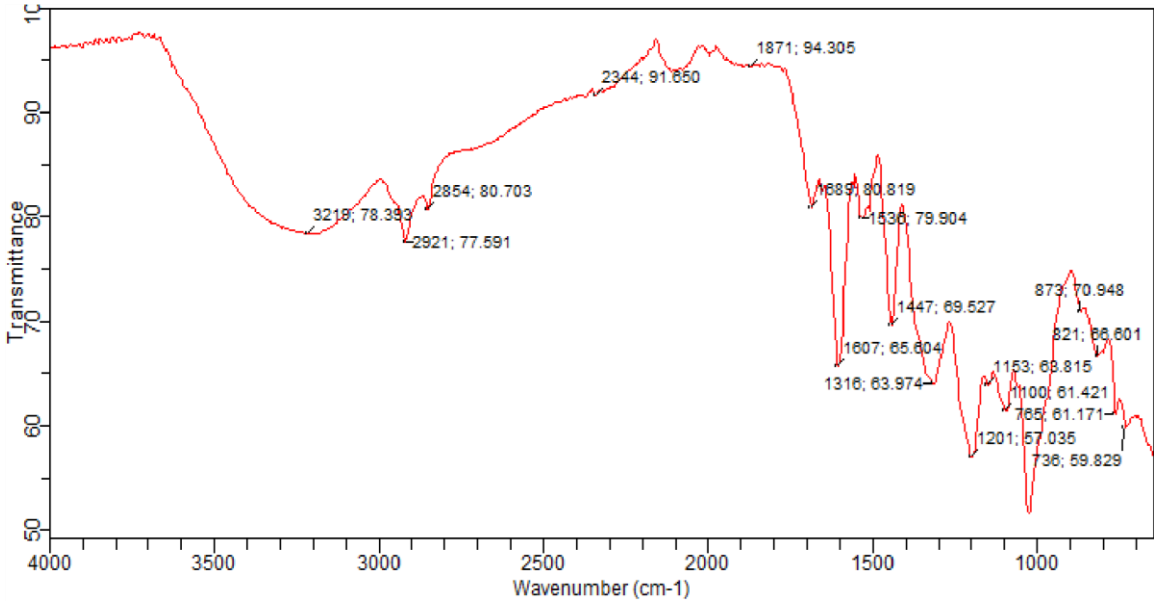

(a) FTIR Spectra of the Ethanol Leaves Extract of *Lannea microcarpa*

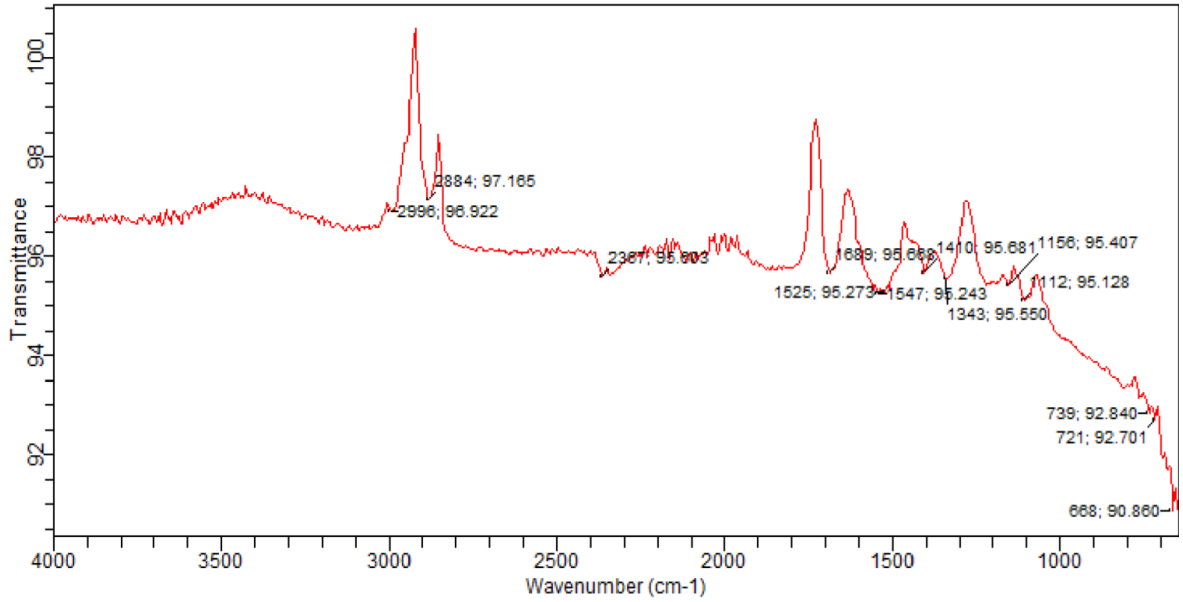

(b) FTIR Spectra of the Corrosion Product of Aluminium in Extract of *Lannea microcarpa*

Figure 5: FTIR Spectra of the studied species.

3.5. Scanning Electron Microscopy

After immersion in the test solutions for 4 hours at 323 K, morphological investigations of the surfaces of uncorroded aluminium and corroded (inhibited and uninhibited acids) specimen were performed using scanning electron microscopy (SEM) (6). The uninhibited system (Fig. 6a) exhibits the most severely corroded surface, which is thoroughly damaged by the presence of cracks, pits, and patches throughout the surface. This is followed by the metals in the inhibited acid Figures (6b-d), which are clearly less corroded than the uninhibited metal. Uncorroded Al metal doesn't have any surface flaws (Fig.6e). This implies that addition of extract of *Lannea microcarpa* leaves to acid solutions protected the Al metal from undergoing severe corrosion by formation of protective layer on the surface through adsorption of the extract on the aluminium surface.

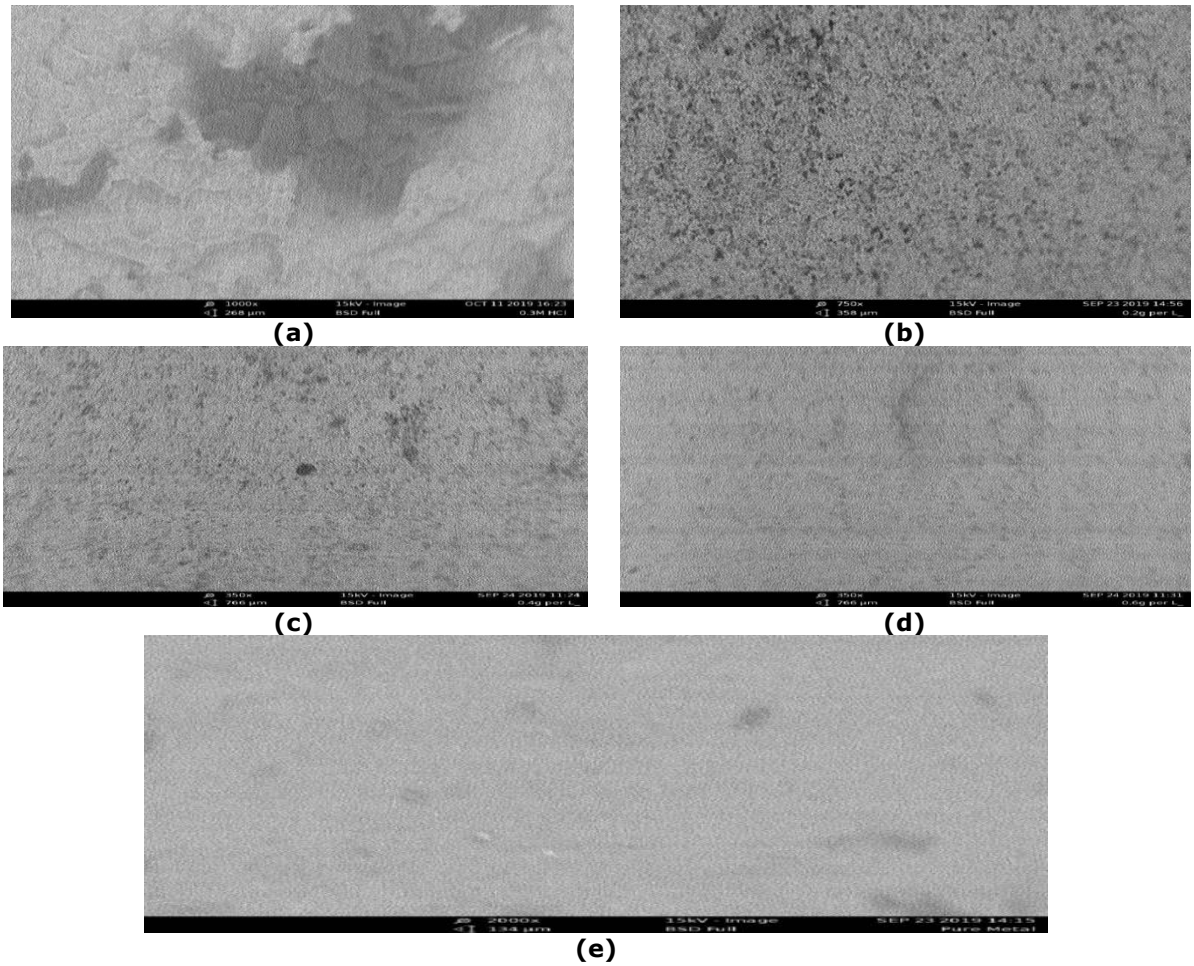

Figure 6: SEM Micrographs of Aluminium Dipped in 0.6 M HCl for (a) 0.0 g/L (Blank) (b) 0.2g/L (c) 0.4 g/L (d) 0.6 g/L of *Lannea microcarpa* Extract, (e) Uncorroded Aluminium.

3.6. Adsorption Isotherms

By creating a thin adsorption layer on the metal surface, inhibitors prevent corrosion on metal surfaces. The degree of inhibitor molecule adsorption on the metal surface has a significant impact on an inhibitor's effectiveness. The adsorption properties of the inhibitors have been used to determine the type of corrosion inhibitors (21). Surface coverage (θ) and inhibitor concentrations can be used to assess the adsorption properties of inhibitors. The interactions between inhibitors and metals are described by a variety of isotherm models. Langmuir, Freundlich, Temkin, Florry-Huggins, and El-Awady isotherm were five of these models that were utilized. The best fit isotherm among them was chosen using the correlation coefficients (R^2) between them. The parameters from the plots of each isotherm at 303, 313 and 323 K are shown in Table 4, and the best fit was determined by taking into account the values of R^2 at all the temperatures. The extract of *Lannea microcarpa* leaves demonstrated strong adherence of the inhibitory process to the Langmuir adsorption isotherm due to its near to unity when compared to the other isotherms, according to the values of R^2 of the investigated isotherms at all temperatures.

The creation of a monolayer adsorbate layer on the adsorbent's outer surface is quantitatively described by the Langmuir adsorption isotherm. The model assumes homogeneous adsorption energies on the surface and prevents adsorbate transmigration in the surface's plane (27). For both chemical and physical adsorption, the Langmuir equation is the ideal isotherm (28). The equilibrium constants K_{ads} values in Table 4 are all positive, indicating a favorable adsorption (29). Equation 5 presents the Langmuir isotherm.

$$C/\theta = 1/K_{ads} + C \quad (5)$$

Where C is the concentration of inhibitor, θ is the surface coverage and K_{ads} the adsorption equilibrium constant

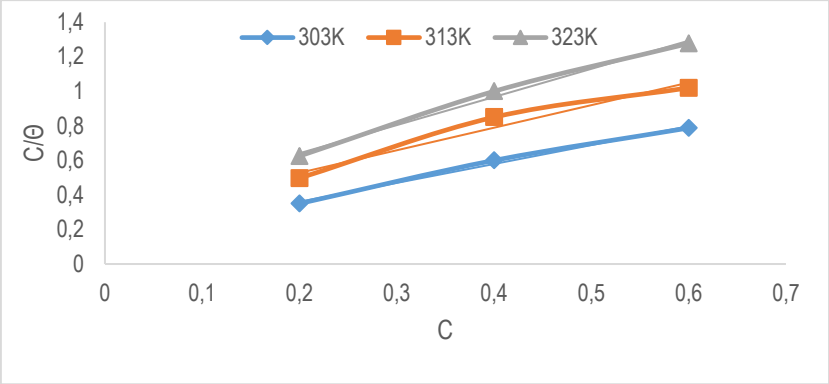

Figure 7: Langmuir Adsorption Isotherm for Al metal in HCl at Different Temperatures.

Table 4: Adsorption Parameters for the Adsorption of *Lannea microcarpa* Extract on Aluminium Surface.

Isotherm	Temperature (K)	Slope	ΔG_{ads} (kJmol^{-1})	R^2	K_{ads}
Langmuir	303	1.09	-15.043	0.9932	7.06
	313	1.38	-13.894	0.9690	3.75
	323	1.63	-13.885	0.9925	3.17
Freundlich	303	0.26	-9.738	0.9883	0.86
	313	0.33	-9.428	0.9395	0.67
	323	0.35	-9.214	0.9968	0.56
Temkin	303	0.39	-22.579	0.9777	140.48
	313	0.37	-20.919	0.9122	55.74
	323	0.31	-21.442	0.9876	52.81
Flory-Huggins	303	1.35	-15.460	0.9286	8.33
	313	1.75	-14.268	0.7913	4.33
	323	2.87	-14.921	0.9686	4.66
EL-Awady	303	0.77	-13.894	0.9635	4.47
	313	0.66	-12.043	0.9138	1.84
	323	0.57	-11.187	0.9914	1.16

3.7. Thermodynamic Studies

The free energy of adsorption, ΔG_{ads} was calculated according to the equation (6):

$$\Delta G_{ads} - 2.303RT\log(55.5K_{ads}) \quad (6)$$

ΔG_{ads} is the Gibbs free energy, K_{ads} is the equilibrium constant for adsorption calculated from the intercept of each adsorption isotherm, R is the universal gas constant, T is the system temperature, and 55.5 is the molar concentration of water. For all of the investigated isotherms, the computed values of ΔG_{ads} vary from -2.238 to -22.579 kJmol^{-1}, which is significantly less than the threshold value of -40kJmol^{-1} needed for the mechanism of chemical adsorption to operate (30). As a result, the adsorption of the *Lannea microcarpa* leaf extract on the surface of aluminium is spontaneous and consistent with physical adsorption (31). Table 4 shows the computed values for ΔG_{ads} and K_{ads} for the tested isotherms at 303, 313 and 323 K. The activation energy for the corrosion process was calculated by using the Arrhenius equation 7:

$$\log CR = \log A - \frac{E_a}{2.303RT} \quad (7)$$

Where CR is the corrosion rate of metal, A is Arrhenius pre-exponential factor, E_a is activation energy (minimum energy needed before the corrosion reaction of the metal proceed), R is universal gas constant and T is the temperature of the system.

The activation energies were computed and are shown in Table 5 as a straight line with a slope equal to $-E_a/2.303R$ when the logCR plot versus the reciprocal of absolute temperature from equation 7 is performed. While the E_a found for the blank is 36.121 kJmol^{-1}, the computed values of E_a for the extract range from 53.363 to 54.340 kJmol^{-1}. The computed values of E_a were found to be higher in inhibited aluminium than in blank aluminium, pointing to the possibility of an adsorption coating that is physically electrostatic in nature (32–33).

Table 5: Energy Parameters for the Dissolution of Aluminium in HCl in Absence and Presence of Different Concentrations of *Lannea macrocarpa.*

Extract Conc. (gL^{-1})	**E_a(KJmol^{-1})**	**ΔH_a(kJmol^{-1})**	**ΔS_a(kJmol^{-1})**
0.0 (blank)	36.121	33.575	-0.1296
0.2	54.330	51.544	-0.0754
0.4	54.340	51.726	-0.0759
0.6	54.363	50.711	-0.0804

The values of enthalpy and entropy changes of the corrosion inhibition processes were calculated according the transition state equation:

$$\log\left(\frac{\mathrm{CR}}{T}\right) = \left\{\log\frac{R}{N_a h} + \frac{\Delta S_a}{2.303R}\right\} - \frac{\Delta \mathrm{H_a}}{2.303RT} \quad (8)$$

Where ΔH_a signifies the enthalpy of the corrosion process, ΔS_a denotes the entropy of activation for the corrosion process, N_A is Avogadro's number and h is plank's constant.

The enthalpy and entropy change of activation for the corrosion inhibition process were estimated from the straight line with slope equal to $(-\Delta H_a)/(2.303R)$ and intercept equal to $\log R(N_a h + (\Delta S_a)/(2.303R)$ that results from the plot of CR/T vs reciprocal of absolute temperature, as shown in Table 5. The endothermic nature of the aluminium dissolving process is shown by the positive values of enthalpy change of activation in both the presence and absence of extract (34). While the activated complex in the rate-determining stage represents association rather than dissociation, as shown by the negative values of adsorption entropies, there is a decrease in disorderliness as one moves from reactant to activated complex (35).

4. CONCLUSION

The results of this investigation employing weight loss, electrochemical, SEM, and FTIR demonstrate that the leaves extract of *Lannea microcarpa* efficiently suppresses the corrosion of aluminium under the examined conditions. With a rise in extract concentration but a decrease in corrosion concentration or temperature, the extract's ability to suppress aluminium corrosion increases. Because several phytochemicals were detected in the extract, it was determined that the inhibitory process was of the mixed type by adsorption. Thermodynamic measurements showed that the extract spontaneously and endothermally adhered to the aluminium surface, supporting the physical adsorption process mechanism.

5. CONFLICT OF INTEREST

The authors declare no conflict of interest.

6. ACKNOWLEDGMENTS

The contribution of the staff of Central Laboratory Complex, Bayero University, Kano, Nigeria is highly appreciated in conducting the surface characterization of the aluminium coupon samples.

7. REFERENCES

1. Ayuba AM, Uzairu A, Abba H, Shallangwa GA. Hydroxycarboxylic acids as corrosion inhibitors on aluminium metal: A computational study. J Mater Environ Sci [Internet]. 2018;9(11):3026–34. Available from: <URL>.

2. Umaru U, Ayuba A. Quantum chemical calculations and molecular dynamic simulation studies on the corrosion inhibition of aluminium metal by myricetin derivatives. J New Technol Mater [Internet]. 2020;10(2):18–28. Available from: <URL>.

3. Umar U, Muhammad AA. Computational study of anticorrosive effects of some thiazole derivatives against the corrosion of aluminium. RHAZES Green Appl Chem [Internet]. 2020 Nov 27;10:113–28. Available from: <URL>.

4. Ayuba AM, Abubakar M. Inhibiting aluminium acid corrosion using leaves extract of *Guiera senegalensis*. J Fundam Appl Sci [Internet]. 2021;13(2):634–56. Available from: <URL>.

5. Al-Otaibi MS, Al-Mayouf AM, Khan M, Mousa AA, Al-Mazroa SA, Alkhathlan HZ. Corrosion inhibitory action of some plant extracts on the corrosion of mild steel in acidic media. Arab J Chem [Internet]. 2014 Jul 1;7(3):340–6. Available from: <URL>.

6. Arbonnier M. Arbres, arbustes et lianes des zones sèches d'Afrique de l'Oues [Internet]. Paris; 2009. Available from: <URL>.

7. Marquet M, Jansen PCM. *Lannea microcarpa* Engl. & K. Krause. Prota 3 Dye Tann Tanins. 2005;

8. Awodoyin RO, Olubode OS, Ogbu JU, Balogun RB, Nwawuisi JU, Orji KO. Indigenous fruit trees of tropical Africa: Status, opportunity for development and biodiversity management. Agric Sci [Internet]. 2015 Jan 8;6(1):31–41. Available from: <URL>.

9. Bereket G, Öğretir C, Yurt A. Quantum mechanical calculations on some 4-methyl-5-substituted imidazole derivatives as acidic corrosion inhibitor for zinc. J Mol Struct THEOCHEM [Internet]. 2001 Aug 27;571(1–3):139–45. Available from: <URL>.

10. Tiwari P, Kumar B, Kaur M, Kaur G, Kaur H. Phytochemical screening and extraction: A review. Int Pharm Sci. 2011;1(1):98–106.

11. Matter HAB, Ayad TM, Alkatly AAI. Grape leaves and ziziphus spina-christi, extracts as a green inhibitors corrosion for the carbon steel and oil pipelines in 1M H_2SO_4. Almanara Sci J [Internet]. 2024 May 4;2024(6):124–45. Available from: <URL>.

12. Matter H, Ayad TM. Study the effect of extract berry and mango leaves as a corrosion inhibitor of Cu, carbon steel and oil pipelines. J Pure Appl Sci [Internet]. 2022 Jun 20;21(1):154–64. Available from: <URL>.

13. Awe FE, Idris SO, Abdulwahab M, Oguzie EE. Theoretical and experimental inhibitive properties of mild steel in HCl by ethanolic extract of *Boscia senegalensis*. Slawin AMZ, editor. Cogent Chem [Internet]. 2015 Dec 31;1(1):1112676. Available from: <URL>.

14. Eddy NO, Odoemelam SA, Odiongenyi AO. Ethanol extract of *Musa acuminate* peel as an eco-friendly inhibitor for the corrosion 24 of mild steel in H_2SO_4. Adv Nat Appl Sci [Internet]. 2008;2(1):35–

42. Available from: <URL>.

15. Ayuba AM, Abdullateef A. Corrosion inhibition potentials of *Strichnos spinosa* L. on Aluminium in 0.9 M HCl medium: Experimental and theoretical investigations. Alger J Eng Technol [Internet]. 2020;3:28. Available from: <URL>.

16. Ebenso EE, Eddy NO, Odiongenyi AO. Corrosion inhibitive properties and adsorption behaviour of ethanol extract of *Piper guinensis* as a green corrosion inhibitor for mild steel in H_2SO_4. African J Pure Appl Chem [Internet]. 2008;2(11):107–15. Available from: <URL>.

17. Obi-Egbedi NO, Obot IB. Xanthione: A new and effective corrosion inhibitor for mild steel in sulphuric acid solution. Arab J Chem [Internet]. 2013 Apr 1;6(2):211–23. Available from: <URL>.

18. Hossain N, Asaduzzaman Chowdhury M, Kchaou M. An overview of green corrosion inhibitors for sustainable and environment friendly industrial development. J Adhes Sci Technol [Internet]. 2021 Apr 3;35(7):673–90. Available from: <URL>.

19. Ayuba AM, Auta MA, Shehu NU. View of comparative study of the inhibitive properties of ethanolic extract of *Gmelina arboreaon* corrosion of aluminium in different media. Appl J Environ Eng Sci [Internet]. 2020;6(4):374–86. Available from: <URL>.

20. Krishnaveni K, Ravichandran J. Effect of aqueous extract of leaves of Morinda tinctoria on corrosion inhibition of aluminium surface in HCl medium. Trans Nonferrous Met Soc China [Internet]. 2014 Aug 1;24(8):2704–12. Available from: <URL>.

21. Thilagavathy P, Saratha R. Mirabilis Jalapa flowers extract as corrosion inhibitor for the mild steel corrosion in 1M HCL. IOSR J Appl Chem [Internet]. 2015;8(1):30–5. Available from: <URL>.

22. Udom G, Cookey G, Abia A. The effect of *Acanthus montanus* leaves extract on corrosion of aluminium in hydrochloric acid medium. Curr J Appl Sci Technol [Internet]. 2017 Dec 26;25(2):1–11. Available from: <URL>.

23. Zhao Q, Tang T, Dang P, Zhang Z, Wang F. The corrosion inhibition effect of triazinedithiol inhibitors for aluminum slloy in a 1 M HCl solution. Metals [Internet]. 2017 Feb 5;7(2):44. Available from: <URL>.

24. Khaled KF, Amin MA. Electrochemical and molecular dynamics simulation studies on the corrosion inhibition of aluminum in molar hydrochloric acid using some imidazole derivatives. J Appl Electrochem [Internet]. 2009 Dec 23;39(12):2553–68. Available from: <URL>.

25. Tang H, Sun J, Su D, Huang Y, Wu P. Coumarin as a green inhibitor of chloride-induced aluminum corrosion: theoretical calculation and experimental exploration. RSC Adv [Internet]. 2021 Jul 16;11(40):24926–37. Available from: <URL>.

26. Okafor PC, Osabor VI, Ebenso EE. Eco-friendly corrosion inhibitors: inhibitive action of ethanol extracts of *Garcinia kola* for the corrosion of mild steel in H_2SO_4 solutions. Pigment Resin Technol [Internet]. 2007 Sep 18;36(5):299–305. Available from: <URL>.

27. Fadare OO, Okoronkwo AE, Olasehinde EF. Assessment of anti-corrosion potentials of extract of *Ficus asperifolia*-Miq (Moraceae) on mild steel in acidic medium. African J Pure Appl Chem [Internet]. 2016;10(1):8–22. Available from: <URL>.

28. Eddy NO, Ebenso E. Adsorption and inhibitive properties of ethanol extracts of *Musa sapientum* peels as a green corrosion inhibitor for mild steel in H_2SO_4. African J Pure Appl Chem [Internet]. 2008;2(6):46–54. Available from: <URL>.

29. Nnanna LA, Onwuagba BN, Mejeha IM, Okeoma KB. Inhibition effects of some plant extracts on the acid corrosion of aluminium alloy. African J Pure Appl Chem [Internet]. 2010;4(1):11–6. Available from: <URL>.

30. Prabhu D, Padmalatha R. Corrosion inhibition of 6063 aluminum alloy by *Coriandrum sativum* L seed extract in phosphoric acid medium. J Mater Environ Sci [Internet]. 2013;4(5):732–43. Available from: <URL>.

31. Loto CA. Inhibition effect of tea (*Camellia Sinensis*) extract on the corrosion of mild steel in dilute sulphuric acid. J Mater Environ Sci [Internet]. 2011;2(4):335–44. Available from: <URL>.

32. Awad MI. Eco friendly corrosion inhibitors: Inhibitive action of quinine for corrosion of low carbon steel in 1 M HCl. J Appl Electrochem [Internet]. 2006 Oct 29;36(10):1163–8. Available from: <URL>.

33. Oguzie EE, Adindu CB, Enenebeaku CK, Ogukwe CE, Chidiebere MA, Oguzie KL. Natural products for materials protection: Mechanism of corrosion inhibition of mild steel by acid extracts of *Piper guineense*. J Phys Chem C [Internet]. 2012 Jun 28;116(25):13603–15. Available from: <URL>.

34. Cookey GA, Tambari BL, Iboroma DS. Evaluation of the corrosion inhibition potentials of green-tip forest lily (*Clivia nobilis*) leaves extract on mild steel in acid media. J Appl Sci Environ Manag [Internet]. 2018 Feb 8;22(1):90. Available from: <URL>.

35. Oguzie EE. Corrosion inhibitive effect and adsorption behaviour of *Hibiscus Sabdariffa* extract on mild steel in acidic media. Port Electrochim Acta [Internet]. 2008;26:303–14. Available from: <URL>.